

Synthesis of mesogen-nanoparticle composites by doping 4-decyloxybenzoic acid with substrate-functionalized ZnO nanoparticle

Saurav Paul^a, Bimal Bhushan Chakraborty^a, Kuheli Deb^a, Sudip Choudhury^{a,b,*}

^aDepartment of Chemistry, Assam University, Silchar-788011, India

^bCentre for Soft Matter, Department of Chemistry, Assam University, Silchar-788011, India

Article history:

Received: 4 February 2023 / Received in revised form: 9 May 2023 / Accepted: 15 May 2023

Abstract

Nanomaterials and Mesogenic materials are two important pillars of today's science and technology, in the fields of both material and biological applications. Mesogens or liquid crystals (LC) are self-aggregated anisotropic fluids with long range order, and the nature of self-aggregation largely controls their physical and material properties. Doping of nanomaterials over liquid crystalline matrix can provide valuable tools for development of materials with new or improved properties. In the present work 4-decyloxybenzoic acid is taken as the mesogenic matrix. It is observed that, composite prepared by doping of 4-decyloxybenzoic acid mesogen matrix by ZnO nanoparticle pre-functionalized with the same mesogen, caused a marked alteration in the mesogenic behavior. With 3% doping of matrix pre-functionalized ZnO NP on 4-decyloxy benzoic acid, we could achieve a shift of about 31°C in the N-Iso transition temperature and, a decrease of >10°C for the onset of liquid crystallinity by this method without quenching any of the mesophases exhibited by the pure mesogen. The synthesized materials have been characterized by variable temperature Polarised optical microscopy (POM), DSC, FTIR, XRD, EDX, and TEM. This process may be considered for preparation other nanoparticle-mesogen composites as well. It was observed that, the effect of doping on the transition temperature and enthalpy of 4-Decyloxybenzoic Acid can be significantly enhanced by pre-functionalizing the dopant (ZnO NP) with the substrate molecules and then mixing this substrate functionalized ZnO nanoparticle with the bulk substrate.

Keywords: Mesogen; ZnO; pre-functionalization; FT-IR

1. Introduction

Liquid crystals and metal-oxide nanoparticles composite is a fast-growing field of research for design of new functional materials [1,2]. Liquid crystals are self-aggregated anisotropic fluids that can acquire a range of mesophases while transiting between the isotropic liquid phase and the crystalline solid phase [3]. Therefore, doping of the nanoparticles (NP) over liquid crystalline compounds can provide valuable tools for development of materials with new or improved properties [4, 5,6].

The conjugation of nanoparticles with liquid crystalline molecules were first reported by Kanayama and co-workers [7]. Recently, Katiyar et. al. reported hexanethiol-capped Silver nanoparticles dispersed in 4'-(Octyloxy)-4-biphenylcarbonitrile (a nematic liquid crystal) exhibiting Ag NPs-assisted induced charge transfer by the composite [8]. A good number of works on nanocomposites of Au NP doped mesogen have been reported [9,10,11,12] with efficient enhancement of the material property of the composite. However, as dopant, Metal oxides get major attentions for their capability to adopt different structural geometries that

can exhibit interesting metallic, semiconducting or insulating character [13,14]. Metal oxide doped mesogenic hybrid materials has been reported using iron oxide [15, 16], Bi₄Ti₃O₁₂ [17], BaTiO₃ [18] etc.

For long, 4-n-alkoxybenzoic acids have been used as important model mesogenic series exhibiting multiple mesophases and, also as building blocks for other liquid crystalline compounds. Yet very few works have been reported on the study of dispersion of nanoparticles in 4-n-alkoxybenzoic acids. The nature and extent of interaction between the LC materials and the guest nanoparticle influence the order parameter in the LC substances, consequently controlling mesophases [13], the strong H-bonding between 4-n-alkoxybenzoic acid molecules puts a hurdle for proper dispersion of nanoparticles there. Recently, Madhav and group reported their finding on the effect of dispersion of unmodified ZnO Nanoparticles in 4-decyloxy benzoic acid and 4-propoxy benzoic acid. They observed a change of about 3°C in the N-Iso transition upon 1% doping of ZnO NP on 4-decyloxy benzoic acid [19], and a change of about 7°C in case of 2.5% doping of ZnO NP on p-propoxy benzoic acid [20].

In the present work we report that pre-functionalization of the ZnO NP with alkoxybenzoic acid and then doping on the mesogenic matrix exhibits a marked difference in the

* Corresponding author.

Email: sudip.choudhury@aus.ac.in, sudipch1@gmail.com
<https://doi.org/10.21924/cst.8.1.2023.1125>

mesogenic behavior than the direct doping of the free nanoparticles with the mesogen base. We could achieve a difference of about 31°C in the N-Iso transition temperature with 3% doping of matrix pre-functionalized ZnO NP on 4-decyloxy benzoic acid. Further, a decrease of more than 10°C for the onset of liquid crystallinity has been achieved by this method, which is important towards development of room temperature mesogenic LC-NP composite materials. This additive-free process may be considered for preparation other nanoparticle-mesogen composites as well.

2. Materials and Methods

2.1. Materials

4-Decyloxybenzoic acid (C10 Acid, 98%) and Zinc chloride (99.995%) were purchased from Sigma Aldrich and used as obtained. Other reagents and solvents were procured from Qualigen. Polarized optical microscopy (POM) was done on a Nikon LV100 equipped with Instec Hotstage. FTIR, UV-Visible, powder XRD, TEM were done on Bruker Alpha II, Jasco 700, Rigaku Ultima IV, and Jeol JEE- 2100 equipment respectively.

2.2. Synthesis of Zinc Oxide nanoparticles (ZnO NP) and functionalization with 4-decyloxybenzoic acid

ZnO nanoparticle was prepared following a previously reported method [21] with necessary modification. For this preparation, ZnCl₂ (100 mmol, 1 eq) was dissolved in 50mL methanol under stirring at 800 rpm. A methanolic solution of NaOH was added in dropwise manner till the reaction mixture reaches pH 10. The reaction mixture was allowed to stir for 4 hours at 60°C. A white colloid of ZnO NP appeared at the end of the reaction. The reaction was periodically monitored by UV-Vis spectroscopy.

To functionalize the ZnO NP, a methanolic solution of 4-decyloxybenzoic acid (10 eq) in was added to the methanolic suspension of the synthesized ZnO nanoparticles and kept to stir for 48 hours at room temperature. The white suspension so obtained was subjected to centrifugation followed by cycles of suspension-sonication-centrifugation (three methanolic cycles followed by three aqueous cycles) to remove any free ligand molecules. The white mass was then collected and dried under vacuum to get the target material, 4-n-decyloxybenzoic acid functionalized ZnO NP (ZnOC10) in powder form.

2.3. Preparation of composite of 4-n-decyloxybenzoic acid and 4-n-decyloxybenzoic acid functionalized ZnO NP (ZnOC10+C10)

Composite, ZnOC10+C10: The nanoparticle-mesogen composite of 4-decyloxybenzoic acid (C10 Acid) and 4-n-decyloxybenzoic acid functionalized ZnO nanoparticle (ZnOC10+C10) was prepared by thoroughly mixing C10 Acid with 3% wt of ZnOC10 at the isotropic melt of the former. In this process, the C10 Acid (20mg) was taken on a quartz concave microscope slide and heated above its clearing point (~150 °C) with an Instec Hotstage monitored through microscope. To this melt ZnOC10 (3% w/w) was added and

thoroughly mixed with a sealed glass capillary. The mixture was cooled to room temperature and heated to isotropic state again. The material so obtained after cooling is collected and used for further analysis.

3. Results and Discussion

HR-TEM image of the synthesized ZnO NP (Figure 1a) exhibited formation of the nanoparticles of about 10 nm diameter. The image at Figure 1b shows functionalized ZnO nanoparticle (ZnOC10) with similar size distribution. The EDX trace (Figure 2) of the ZnOC10 nanoparticles detected Zn, C, and O confirming the presence of the functionalizing ligand. The functionalization of the ligand to the nanoparticle surface further confirmed from the FT-IR spectroscopy.

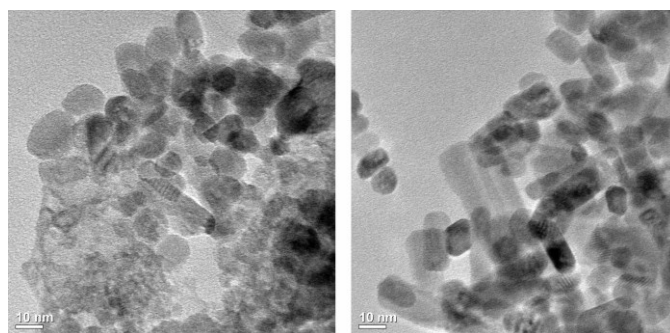


Fig. 1. TEM images of (a) ZnO NPs (left), (b) ZnOC10 NPs (right)

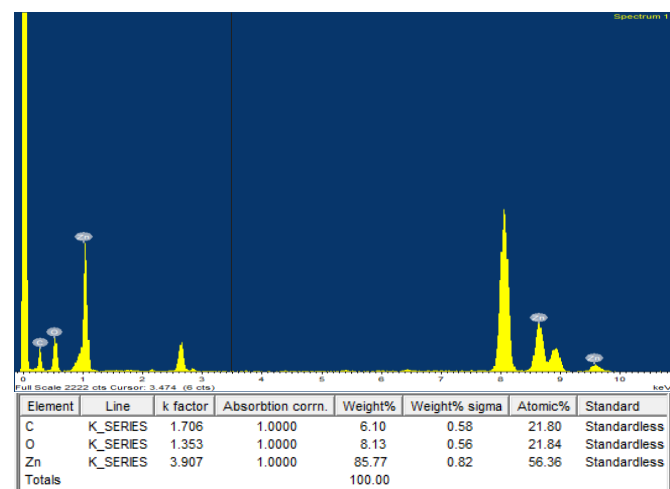


Fig. 2. EDX scan of ZnOC10 NPs

The FT-IR spectral data of ZnO NP, 4-decyloxybenzoic acid (C10 Acid), and ZnOC10 are overlaid in Figure 3. Free ZnO nanoparticles exhibited strong $\nu_{\text{Zn-O}}$ band at 487 cm⁻¹. The free ligand, 4n-decyloxybenzoic acid exhibited the characteristic $\nu_{\text{C-H(alkyl)}}$ bands at 2914 and 2850 cm⁻¹ for the alkoxy end chain, and $\nu_{\text{C=O}}$ band at 1673 cm⁻¹. The IR spectrum of the functionalized material, ZnOC10 bears the signature of both the components ZnO NP and 4-decyloxybenzoic acid indicating their co-existence in the material. There was no change in the band position of C-H stretching (2914 and 2850 cm⁻¹) and etheric C-O stretching (1250 cm⁻¹) between 4-decyloxybenzoic acid and ZnOC10 confirming the expected non-participation of the alkoxy side chain region of the alkoxybenzoic acid for ligand grafting on the metal oxide nanoparticle surface. However, at the same

time the marked shift of C=O stretching from 1673 cm^{-1} (in 4-decyloxybenzoic acid) to 1622 cm^{-1} (in ZnOC10) infers the attachment of the ligand on the surface of the ZnO NP through the carboxylic acid group of the former, confirming the successful functionalization of 4-decyloxybenzoic acid on ZnO nanoparticle.

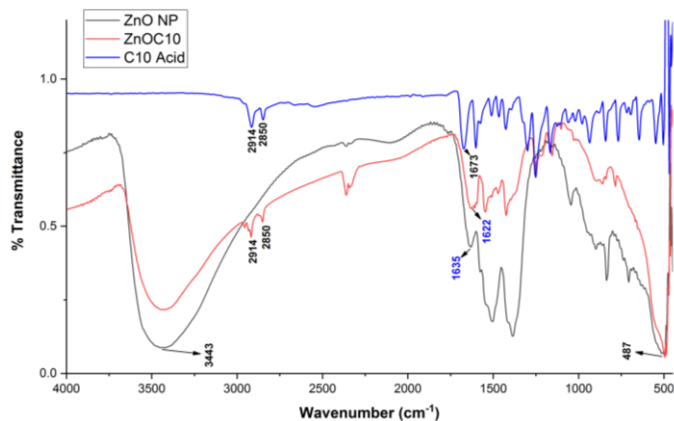


Fig. 3. FT-IR spectra of ZnO NP, ZnOC10, and C10 acid

Differential Scanning Calorimetry (DSC) of the composite was done to study the phase transition behavior and compared with that of the pure mesogen. The mesogenic matrix, Decyloxybenzoic acid exhibited characteristic phases transitions in the DSC thermogram (Figure 4a). However, in case of the composite ZnOC10+C10, where the mesogenic base material (C10 Acid) was doped with ZnO nanoparticle pre-functionalized with the same compound, the consequence was dramatic. The composite, ZnOC10+C10 though exhibited the same number of transitions in the heating cycle (Figure 4b) but with distinct difference in the transition temperature compared to 4-Decyloxybenzoic acid. During the heating cycle, ZnOC10+C10 entered liquid crystal phase at 87 °C, and exhibited clearing temperature of 111°C. Each of the transitions was of considerably low transition enthalpy and larger FWHM/Peak height ratio compared to those of pure C10 Acid. Like the pure mesogen, the composite also exhibited Cr1-> Cr2 transition with the highest enthalpy change. Apart from the Cr/Cr transition, it was the clearing enthalpy (at 111°C) that was the maximum in case of the composite, whereas, the Cr/SmA transition enthalpy was highest in case of the pure mesogen (Figure 4). The enthalpy of Sm->N transition was almost equal to that of N->Iso transition in case of Decyloxybenzoic acid, but upon the incorporation of the ZnOC10 the Sm->N transition enthalpy reduced to about 1/3rd of N->Iso transition. This seems to be due to the modification of short-range molecular arrangement in the mesophase owing to the association of nanoparticles (functionalized with same the matrix material) and the free bulk material. Due to functionalization, the ZnOC10 nanoparticles could easily homogenized with the mesogen. The remarkable shift in the Melting point (~15 °C) and Clearing point (~31 °C) indicate notable interaction between the ZnOC10 and bulk C10 acid. Such interaction also resulted in forced orientation of the nanoparticles in the bulk matrix as evidenced by XRD (discussed later). However, the insertion of nanoparticles in the intercalated region of the bulk C10 acid would hinder ease of crystallization of C10 Acid thereby decreasing both the

Melting point and the delta H, resulting in onset of mesophase at a much lower temperature. The presence of ZnOC10 would strongly interfere with the layered formation of Smectic phase due to its longer effective length compared to free C10 Acid molecules. Therefore, it would be difficult to maintain the layered molecular arrangement which is integral necessity of Smectic mesophase. As Nematic phase does not have layered arrangement, the Smectic to nematic transition would be much less energy demanding. This resulted in very low transition enthalpy for the Smectic to Nematic transition of the composite.

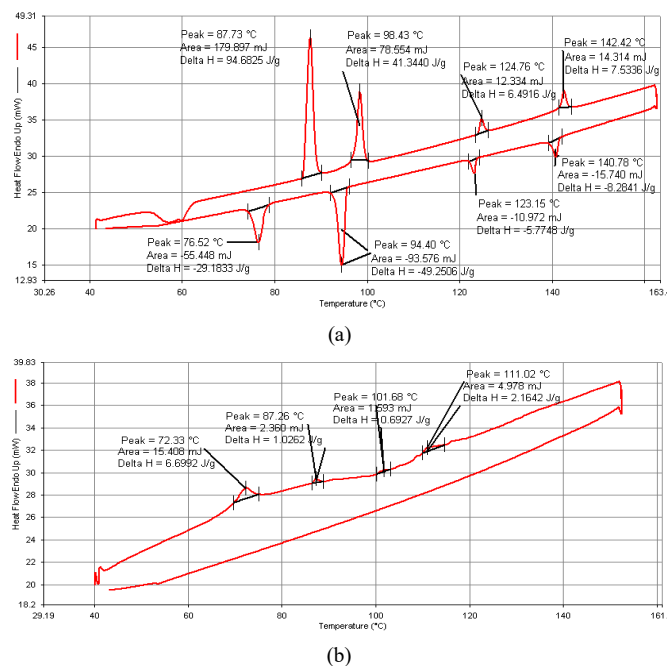


Fig. 4. DSC thermogram of (a) C10 acid, (b) ZnOC10+C10 composite

Variable temperature Polarized Optical Microscopy (POM) study was done with the pure mesogen (C10 Acid), and the composite (ZnOC10+C10) and were in agreement with the DSC thermogram. The C10 Acid exhibited characteristic transitions showing Cr1, Cr2, SmA, N, and Iso phases in the heating and cooling cycles (Table 1).

Table 1. Phase transitions of the pure mesogen and the composite

Material	DSC/ POM	Cycle	Phase Transitions (°C)			
			Cr1 - Cr2	Cr2 - SmA	SmA - N	N - Iso
C10 Acid	DSC	Heating	87.7	98.4	124.8	142.4
		Cooling	76.5	94.4	123.1	140.8
	POM	Heating	88.2	99.0	125.2	143.0
		Cooling	-	93.8	123.0	140.0
ZnOC10+C10	DSC	Heating	72.3	87.3	101.7	111.0
		Cooling	-	-	-	-
	POM	Heating	-	85.0	103.0	112.8
		Cooling	-	84.2	101.0	112.1

The composite, ZnOC10+C10, showed onset of melting at 85 °C, and moved to Isotropic state at 112.8°C with exhibition of SmA and N phases in between. During cooling cycle, Nematic phase slowly re-appeared from isotropic melt in the form of nematic droplet at 112.1 °C followed by SmA at 101

°C. The transitions details are presented in Table 1. POM images of C10 Acid and ZnOC10+C10 are presented in Figure 5.

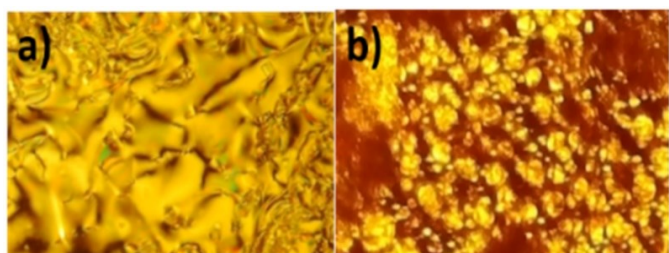


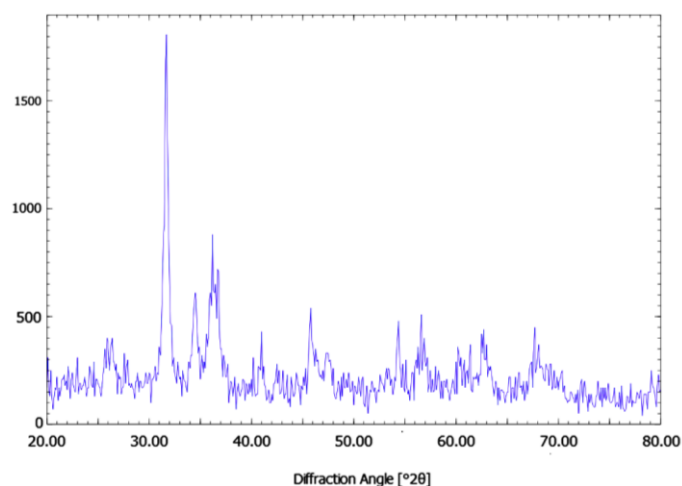
Fig. 5. POM images (taken with crossed polarizers) of a) nematic texture of C10 acid at 135°C, b) nematic texture of 3% ZnOC10 doped in C10 acid, 107°C.

The XRD pattern of ZnO NP and ZnOC10+C10 composite material are presented in Figure 6. The X-ray diffractogram of ZnO NP exhibited characteristic peaks corresponding to (100) at 31.5, (002) at 34.5, (101) at 36.0, (102) at 45.8, (110) at 56.8, (112) at 68.0 ° 2theta (Figure 6(a)) and in agreement with JCPDS-36-1451 [22]. The diffraction pattern of the composite, ZnOC10+C10 was recorded at 105 °C when the material was at nematic phase (Figure 6(b)). The sample was taken in the platinum holder supplied with the equipment. After reaching the intended temperature of 105 °C, it was held at that temperature for 2min for thermal equilibration before the XRD scanning. The XRD pattern so obtained exhibited a broad peak at 20 ° 2theta, indicating fluidic nature of the mesophase. The presence of sharp peaks at 2theta (degree) of 31.5, 46.1, 56.2 are attributed to the (100), (102), (110) planes of the ZnO nanoparticles. The peaks at 39.7 and 45.1 appeared from the (111) and (200) planes of Platinum holder surface respectively. The high intensity of diffraction from the (100) plane compared to those of (002) at 34.2 ° and (101) at 36.0 ° 2theta seems to be due to high preferential orientation of the ZnO nanoparticle core enforced by self-assembly of the nematic dispersing medium.

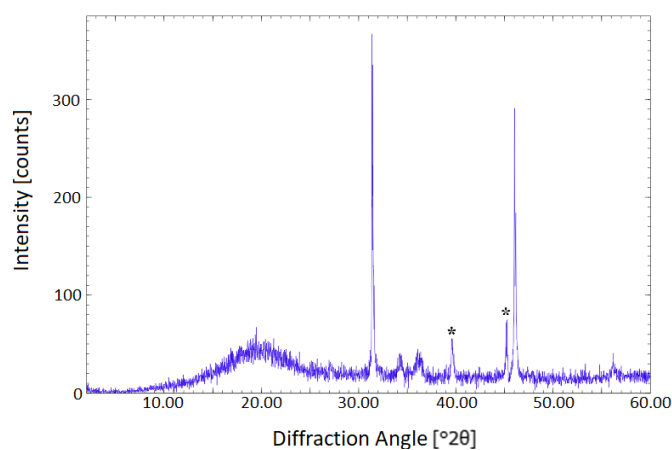
The Wurtzite form of ZnO possess a hexagonal structure (space group $C6_{3mc}$) with polar surfaces commonly at the basal plane, viz, positively charged Zn-[0001] and negatively charged O-[000 $\bar{1}$] surfaces. Such polar planes cause a divergence in surface energy at different planes of its unit cell and a spontaneous polarization along the c-axis [23]. As ZnO unit cell exhibited different kinetic parameters at different crystal planes, the 4-decyloxybenzoic acid molecules preferred the polar surfaces of ZnO for functionalization. Keeping the different bonding preferences of Zn and O atoms, Wahl et al [24] had suggested through DFT study that, the polar O-[000 $\bar{1}$] may get stabilized either by depleting oxygen from the surface or by adsorption of hydrogen. The carboxylic acid group in the mesogenic compound 4-decyloxybenzoic acid is thus expected to get attached to both the polar surfaces (Figure 7a); with Zn-[0001] surface by carbonyl oxygen, and with O-[000 $\bar{1}$] surface by hydroxyl group (seemingly through H-bonding or O...H...O association).

Importantly, such preferential functionalization at the basal surfaces will lead to orientation of the functionalized ZnO nanoparticle in such a way that its polar c-axis aligns parallel to the molecular director of the mesophase. Such self-assembly caused exposure the (100) plane resulting the high

intensity peak at 31.5 ° 2theta, suppressing the diffraction from (002) and (101) planes (Figure 7b).



(a)



(b)

Fig. 6. (a) XRD pattern of ZnO NP (top), (b) XRD pattern of the composite, ZnOC10+C10 recorded at 105 °C (bottom). Peaks marked with (*) were from Pt holder

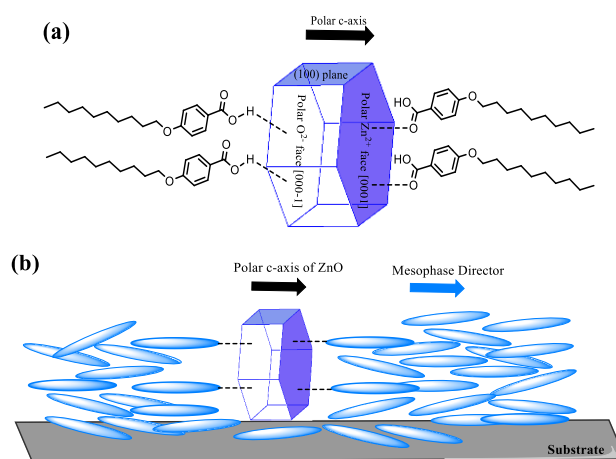


Fig. 7. Schematic presentation of (a) Proposed scheme of functionalization of 4-decyloxybenzoic acid on ZnO polar faces, (b) Alignment of the functionalized ZnO NP under the influence of bulk 4-decyloxybenzoic acid

4. Conclusion

Doping of mesogen with nanomaterials is being explored

to tune the material properties of the individual components. The present work demonstrated that the pre-functionalization of nanomaterials with the same mesogenic molecules before adding it to the bulk mesogenic dispersion medium has a profound effect on the molecular arrangement and their thermodynamics. The plausible mode of functionalisation and its effect on the molecular self-assembly of the mesogenic composite has been discussed. As most of the mesogenic materials exhibit liquid crystalline phase much above room temperature, the present technique may be studied as an additional tool to increase the interaction between the nanoparticle and the mesogenic substrate significantly, thereby better tuning of the onset of mesogenicity in other LC-NP composites as well.

Acknowledgements

The authors express thankfulness to DST-FIST program of Chemistry Department, Assam University for XRD, and SAIF, Shillong for TEM facility. DST-INSPIRE Fellowship to SP and KD, and UGC Fellowship to BBC are thankfully acknowledged.

References

1. S. Orlandi, E. Benini, I. Miglioli, D. R. Evans, V. Reshetnyak, and C. Zannoni, *Doping liquid crystals with nanoparticles. A computer simulation of the effects of nanoparticle shape*, Phys. Chem. Chem. Phys., 18 (2016) 2428-2441
2. C. Hamon, E. Beaudoin, P. Launois, and E. Paineau, *Doping Liquid Crystals of Colloidal Inorganic Nanotubes by Additive-Free Metal Nanoparticles*, J. Phys. Chem. Lett., 12 (2021) 5052-5058
3. Y. Shen and I. Dierking, *Perspectives in Liquid-Crystal-Aided Nanotechnology and Nanoscience*, Applied Sciences, 9 (2019) 2512
4. G. Yadav, M. Kumar, A. Srivastava, and R. Manohar, *SiO₂ nanoparticles doped nematic liquid crystal system: An experimental investigation on optical and dielectric properties*, Chinese Journal of Physics, 57 (2019) 82-89
5. F. Ahmad, M. Luqman, and M. Jamil, *Advances in the metal nanoparticles (MNPs) doped liquid crystals and polymer dispersed liquid crystal (PDLC) composites and their applications - a review*, Molecular Crystals and Liquid Crystals, 731 (2021) 12055
6. Y. Shen and I. Dierking, *Perspectives in Liquid-Crystal-Aided Nanotechnology and Nanoscience*, Applied Sciences, 9 (2019) 2512
7. N. Kanayama, O. Tsutsumi, A. Kanazawa, and T. Ikeda, *Distinct thermodynamic behaviour of a mesomorphic gold nanoparticle covered with a liquid-crystalline compound*, Chem. Commun., (2001) 2640-2641
8. R. Katiyar et al., *Silver nanoparticles dispersed in nematic liquid crystal: an impact on dielectric and electro-optical parameters*, J Theor Appl Phys, 14 (2020) 237-243
9. S. Lalik et al., *Nanocomposites Based on Antiferroelectric Liquid Crystal (S)-MHPOBC Doping with Au Nanoparticles*, Molecules, 27 (2022) 3663
10. S. Mischler, S. Guerra, and R. Deschenaux, *Design of liquid-crystalline gold nanoparticles by click chemistry*, Chem. Commun., 48 (2012) 2183
11. Kumar, J. Prakash, D. S. Mehta, A. M. Biradar, and W. Haase, *Enhanced photoluminescence in gold nanoparticles doped ferroelectric liquid crystals*, Appl. Phys. Lett., 95 (2009) 23117
12. P. Tripathi, M. Mishra, S. Kumar, and R. Dhar, *Thermodynamic study of a plastic columnar discotic material 2, 3, 6, 7, 10, 11-hexabutyloxytriphenylene dispersed with gold nanoparticles under elevated pressure*, J Therm Anal Calorim, 129 (2017) 315-322
13. Chandran et al., *Preparation and characterization of MgO nanoparticles/ferroelectric liquid crystal composites for faster display devices with improved contrast*, J. Mater. Chem. C, 2 (2014) 1844
14. M. S. Chavali and M. P. Nikolova, *Metal oxide nanoparticles and their applications in nanotechnology*, SN Appl. Sci., 1 (2019) 607
15. O. V. Kovalchuk et al., *Dielectric and electrical properties of nematic liquid crystals 6CB doped with iron oxide nanoparticles. The combined effect of nanodopant concentration and cell thickness*, Journal of Molecular Liquids, 366 (2022) 120305
16. R. Cimbala et al., *Dielectric response of a hybrid nanofluid containing fullerene C60 and iron oxide nanoparticles*, Journal of Molecular Liquids, 359 (2022) 119338
17. Anu, D. Varshney, K. Yadav, J. Prakash, H. Meena, and G. Singh, *Tunable dielectric and memory features of ferroelectric layered perovskite Bi₄Ti₃O₁₂ nanoparticles doped nematic liquid crystal composite*, Journal of Molecular Liquids, 369 (2023) 120820
18. L. Scolari et al., *Nanoparticles Doped Liquid Crystal Filled Photonic Bandgap Fibers*, AIP Conference Proceedings, 1055 (2008) 29-32
19. B. T. P. Madhav, P. Pardhasaradhi, R. K. N. R. Manepalli, P. V. V. Kishore, and V. G. K. M. Pisipati, *Image enhancement using virtual contrast image fusion on Fe₃O₄ and ZnO nanodispersed decyloxy benzoic acid*, Liquid Crystals, 42 (2015) 1329-1336
20. P. Jayaprada et al., *Effect of ZnO nanoparticles dispersed in liquid crystalline p-n-propoxy/propyl benzoic acids and mixtures – optical studies*, Molecular Crystals and Liquid Crystals, 689 (2019) 12328
21. M-A. Gatou, N. Lagopati, I-A. Vagena, et al., *ZnO Nanoparticles from Different Precursors and Their Photocatalytic Potential for Biomedical Use*, Nanomaterials, 13 (2022) 122
22. T.M. Elmersi, M.H. Elsayed, M.F. Bakr, *Enhancing the removal of methylene blue by modified ZnO nanoparticles: kinetics and equilibrium studies*, Can J Chem, 95 (2017) 590
23. Z. L. Wang, *Zinc oxide nanostructures: growth, properties and applications*, J. Phys.: Condens. Matter, 16 (2004) R829-R858
24. R. Wahl, J. V. Lauritsen, F. Besenbacher, and G. Kresse, *Stabilization mechanism for the polar ZnO(0001) surface*, Phys. Rev. B, 87 (2013) 85313